Michel Le Hir · Ivan Hegyi
Dominique Cueni-Loffing · Johannes Loffing
Brigitte Kaissling

Characterization of renal interstitial fibroblast-specific protein 1/S100A4-positive cells in healthy and inflamed rodent kidneys

Abstract Fibrosis is considered as a central factor in the loss of renal function in chronic kidney diseases. The origin of fibroblasts and myofibroblasts that accumulate in the interstitium of the diseased kidney is still a matter of debate. It has been shown that accumulation of myofibroblasts in inflamed and fibrotic kidneys is associated with upregulation of fibroblast-specific protein 1 (FSP1, S100A4), not only in the renal interstitium but also in the injured renal epithelia. The tubular expression of FSP1 has been taken as evidence of myofibroblast formation by epithelial–mesenchymal transition (EMT). The identity of FSP1/S100A4 cells has not been defined in detail. We originally intended to use FSP1/S100A4 as a marker of putative EMT in a model of distal tubular injury. However, since the immunoreactivity of FSP1 did not seem to fit with the distribution and shape of fibroblasts or myofibroblasts, we undertook the characterization of FSP1/S100A4-expressing cells in the interstitium of rodent kidneys. We performed immunolabeling for FSP1/S100A4 on thin cryostat sections of perfusion-fixed rat and mouse kidneys with peritubular inflammation, induced by thiazides and glomerulonephritis, respectively, in combination with ecto-5′-nucleotidase (5′NT), recognizing local cortical peritubular fibroblasts, with CD45, MHC class II, CD3, CD4 and Thy 1, recognizing mononuclear cells, with alpha smooth muscle actin (αSMA), as marker for myofibroblasts, and vimentin for intracellular intermediate filaments in cells of mesenchymal origin. In the healthy interstitium of rodents the rare FSP1/S100A4+ cells consistently co-expressed CD45 or lymphocyte surface molecules. Around the injured distal tubules of rats treated for 3–4 days with thiazides, FSP1+/S100A4+, 5′NT+, αSMA+, CD45+ and MHC class II+ cells accumulated. FSP1+/S100A4+ cells consistently co-expressed CD45. In the inflamed regions, αSMA was co-expressed by 5′NT+ cells. In glomerulonephritic mice, FSP1+/S100A4+ cells co-expressed Thy 1, CD4 or CD3. Thus, in the inflamed interstitium around distal tubules of rats and of glomerulonephritic mice, the majority of FSP1+ cells express markers of mononuclear cells. Consequently, the usefulness of FSP1/S100A4 as a tool for detection of (myo)fibroblasts in inflamed kidneys and of EMT in vivo is put into question. In the given rat model the consistent co-expression of αSMA and 5′NT suggests that myofibroblasts originate from resident peritubular fibroblasts.

Keywords Kidney · Fibroblast · Myofibroblast · Epithelial mesenchymal transition · Thiazide · FSP1 · S100A4 · Renal interstitium

Ivan Hegyi and Michel Le Hir contributed equally to the study

M. Le Hir · D. Cueni-Loffing · B. Kaissling (✉)
Anatomical Institute,
Division of Vegetative Anatomy,
University of Zurich, Winterthurerstr. 190,
8057 Zurich, Switzerland
E-mail: bkaissl@anatom.unizh.ch
Tel.: +41-1-6355320
Fax: +41-1-6355702

I. Hegyi
Department of Pathology,
Institut für Klinische Pathologie,
University of Zürich, Zurich,
Switzerland

J. Loffing
Institut d'Anatomie Université de Fribourg,
Zurich, Switzerland

Introduction

In the kidney, inflammatory and fibrotic lesions are characterized by the occurrence of myofibroblasts in the peritubular interstitium. Myofibroblasts are absent from healthy kidneys. They differ from fibroblasts (Bulger and Nagle 1973; Kaissling et al. 1996; Lemley and Kriz 1991) by their high production of extracellular matrix (ECM) and expression of vimentin as well as α smooth muscle actin (αSMA). The latter is usually regarded as a molecular marker for myofibroblasts (Desmouliere et al.

2003). The accumulation of myofibroblasts in a diseased kidney is considered as an important factor in the development of chronic renal failure (Abbate et al. 2002; El-Nahas 2003; Strutz and Neilson 2003; Zeisberg et al. 2001).

It is widely accepted that, under the stimulus of inflammatory cytokines, local fibroblasts are transformed to myofibroblasts (Desmouliere et al. 2003; Diamond et al. 1995; Phan 2002; Sartore et al. 2001; Short et al. 2004). For the kidney, however, an attractive and provocative alternative hypothesis has been put forward, that of "epithelial mesenchymal transition" (EMT). During embryonic development EMT is vital for morphogenesis, whereas, in adults, it is linked to tumor metastasis and tissue repair (Kang and Massague 2004). During the process of EMT, epithelial cells loose their cell polarity and cell–cell contacts and undergo dramatic remodeling of the cytoskeleton (Thiery 2002). The cells acquire expression of mesenchymal components (e.g., αSMA, vimentin) and manifest a migratory phenotype (Kang and Massague 2004). The EMT program also includes the acquisition of mesenchymal functions (Thiery 2002). Because renal epithelia develop by mesenchymal–epithelial transformation from the mesenchymal metanephrogenic blastema, a reversal of this pathway, from epithelia back to cells with mesenchymal properties, seems conceivable (Herzlinger 2002).

In inflamed and fibrotic kidneys the coincidence of upregulation of "fibroblast-specific protein 1" (FSP1) in the interstitium and in injured tubular epithelia has been taken as crucial evidence of tubular epithelial cells undergoing EMT and their subsequent colonization of the interstitial space as (myo)fibroblasts (Iwano and Neilson 2004; Kalluri and Neilson 2003; Liu 2004; Strutz and Neilson 2003). In healthy kidneys, antibodies against FSP1 are bound to very few interstitial cells. By contrast, in inflamed kidneys, the number of FSP1-positive cells in the peritubular space is markedly increased, and the structurally altered tubular cells reveal a diffuse cytoplasmatic binding of the antibody, suggesting EMT. Therefore, the FSP1 protein is used as a tool in order to disclose EMT and to detect myofibroblasts in diseased kidneys (Iwano and Neilson 2004; Kalluri and Neilson 2003). Outside the field of renal pathology the protein is mostly known as S100A4 (Barraclough 1998; Mazzucchelli 2002).

We had previously observed that treatment of rats with the thiazide diuretic metolazone provokes a very specific and reproducible pattern of injury in the early portion of the distal convoluted tubule (DCT) (Loffing et al. 1996). On the third day of treatment the tubular cells seemed to loose their epithelial characteristics. At the same time the interstitium surrounding the damaged tubules became inflamed and cells with the morphology of myofibroblasts could be found. The simultaneity of the dedifferentiation of the epithelium and of the appearance of myofibroblast-like cells suggested that EMT might take place. In the present study we undertook a characterization of the interstitial cells in that model of distal tubular injury. We used antibodies against FSP1 in order to disclose a possible transdifferentiation of distal tubular cells into (myo)fibroblasts.

Our data show that FSP1 is consistently associated with a subpopulation of mononuclear cells but not with fibroblasts or myofibroblasts. Thus, FSP1 is not qualified for detection of fibroblasts and myofibroblasts, and the conclusions of several studies on the role of EMT in the genesis of myofibroblasts must be put into question.

Material and methods

Experimental models for peritubular inflammation

We used the formerly described experimental model of thiazide treatment in rats (Loffing et al. 1996), which provokes massive injury of epithelial cells in the DCT exclusively. The lesion of the DCT epithelium is accompanied by a peritubular inflammatory reaction.

Briefly, we applied to male rats (~160 g) by osmotic minipump (Alzet 2ML1) a daily dose of 4 mg metolazone/kg body weight (ICN Biomedicals, Aurora, Ohio, USA), dissolved in PEG 300. In controls, the pumps contained PEG 300 only. All animals had free access to food and the choice between tap water and an electrolyte solution (0.8% NaCl + 0.1% KCl).

In addition, we used perfusion-fixed kidneys of healthy and of glomerulonephritic mice, as described formerly (Le Hir et al. 2001). Briefly, for induction of glomerulonephritis, mice were immunized against rabbit immunoglobulins on day 0. On day 6 they received an i.v. injection of rabbit antiglomerular basement membrane serum. They were perfusion-fixed 6 days later.

The experimental protocols were approved by the Cantonal Veterinary Office of Zurich.

Fixation and tissue treatment

After 3–4 days of treatment three control and five metolazone-treated rats were anesthetized by an i.p. injection of pentobarbital (100 mg/kg body weight) and fixed by vascular perfusion (Dawson et al. 1989). The fixative contained 3% paraformaldehyde (PFA), 0.01% glutardialdehyde (GA) and 0.5% picric acid. The fixatives were dissolved in a 3:2 mixture of 0.1 M cacodylate buffer (pH 7.4, added with sucrose, final osmolality 300 mosmol) and 4% hydroxyl ethyl starch (HES; Fresenius) in 0.9% NaCl. The kidneys were fixed for 5 min and then rinsed by vascular perfusion with 0.1 M cacodylate buffer for 5 min.

Some tissue slices were post-fixed for at least 24 h by immersion in the above fixative supplemented with 0.5% glutardialdehyde, and embedded in epoxy resin according to routine procedures. One-micrometer sections were studied by light microscopy.

The remaining kidney tissue was used for immunofluorescence studies. Two-millimeter-thick coronal slices of kidney were frozen in liquid propane cooled by liquid nitrogen and cut into 4-μm-thick cryostat sections. For preparation of semi-thin (1 μm) cryostat sections small tissue pieces were infiltrated with PVP-sucrose prior to being frozen in liquid propane.

Immunostaining

After pretreatment in 10% normal goat serum in PBS, the cryostat sections were incubated overnight in a humidified chamber at 4°C with the primary antibodies (listed in Table 1), diluted in PBS-1% BSA.

Binding sites of the primary antibodies were revealed with Cy3-conjugated donkey-anti-rabbit IgG or fluorescein isothiocyanate (FITC)-conjugated swine anti-rabbit, with a FITC-conjugated goat-anti-mouse IgG or Cy3-conjugated rat anti-mouse IgG (all Jackson Immuno Research Laboratories, West Grove, Pa., USA). For nuclear staining, 4′,6-diamidino-2-phenylindole (DAPI; Sigma, St. Louis, Mo., USA) was added to the working dilution of the second antibodies. Double labeling was performed using cocktails of mouse and rabbit or rat and rabbit primary antibodies and of the respective second antibodies.

Cover slips were applied to the sections, using DAKO-Glycergel (Dakopatts) to which 2.5% 1,4-diazabicyclo[2,2,2]octane (DABCO; Sigma) was added as fading retardant.

The specificity of all primary antibodies had been established previously (Dawson et al. 1989; Gandhi et al. 1990; Strutz et al. 1995). For control of unspecific binding of secondary antibodies we did control incubations by omitting the primary antibody. These control experiments were negative. Sections were studied by epifluorescence with a Polyvar microscope (Reichert Jung, Vienna, Austria). Images were acquired with a charge-coupled device camera (Visicam 1280, Visitron Systems, Puching, Germany) and processed by Image-Pro and Photoshop software.

Results

The peritubular interstitium is the narrow space between the basement membranes of tubules and capillaries. Fibroblasts constitute its cellular scaffolding. They are attached to the basement membranes of capillaries and tubules. Their fine interconnected processes form a complex meshwork extending through the cortex and narrowly enwrap cells of the immune system (Kaissling et al. 1996; Kaissling and Le Hir 1994). In conventionally immersion-fixed renal tissue, the capillaries and the interstitial space are collapsed. Thus, due to cellular superposition the various cell types (endothelial cells, fibroblasts, and dendritic and mononuclear cells) are merely distinguishable from each other. In the present study we circumvented these problems by using vascular perfusion fixation, resulting in patent tubular and capillary lumina and in preservation of the interstitial space. In addition, when needed, we used thin cryosections (1 μm) in order to increase the spatial resolution.

Focal peritubular inflammation associated with injured distal tubules in thiazide-treated rats

In rats, treatment with the thiazide-like diuretic metolazone provokes massive cell injury in the early portion of the DCT (Loffing et al. 1996). After 3 days the DCT cells lose their usual organization and their polarization with respect to plasma membrane proteins (Loffing et al. 1996). The tubular lumen is often occluded, and the epithelial lining contains frequent apoptotic cells (Fig. 1a). After 4 days most DCT profiles are lined by flat cells with a light cytoplasm, sparse cell organelles and large nuclei. Epithelial cells desquamating into the tubular lumen are seen (Fig. 1b). The damaged tubules are enveloped by thick layers of cells comprising mononuclear cells, fibroblasts (Fig. 1a), and cells with fusiform profiles probably representing myofibroblasts (Fig. 1 a, b). In overviews diseased DCT profiles are obvious by the prominent accumulation of vimentin (fig 1c) and αSMA (Fig. 1d) in the adjacent interstitium.

Table 1 List of primary antibodies

Primary antibodies	Host	Source	Reference
Fibroblast specific antigen 1 (FSP1)	Rabbit	Courtesy F. Strutz	Strutz et al. (1995)
S100A4	Rabbit	Dako, Glostrup, Denmark	
Ecto-5′nucleotidase (5′NT)	Rabbit	M. Le Hir	Dawson et al. (1989)
Ecto-5′nucleotidase (5′NT)	Mouse	BD Biosciences, Franklin Lakes, N.J., USA	Gandhi et al.(1990)
Alpha smooth muscle actin (αSMA)	Mouse	Dako, Glostrup, Denmark	
Vimentin	Mouse	Chemicon, Single Oak Drive, USA	
Common leucocyte antigen CD 45	Mouse	Readysystem, Bad Zurzach, Switzerland	
CD3	Rat	Clone KT3	
CD4	Rat	Clone GK1.5	
Thy 1	Rat	Clone 30-H12	
Rat MHC class II	Mouse	Clone OX 6	
Mouse MHC class II	Rat	Clone M5/114.15.2	

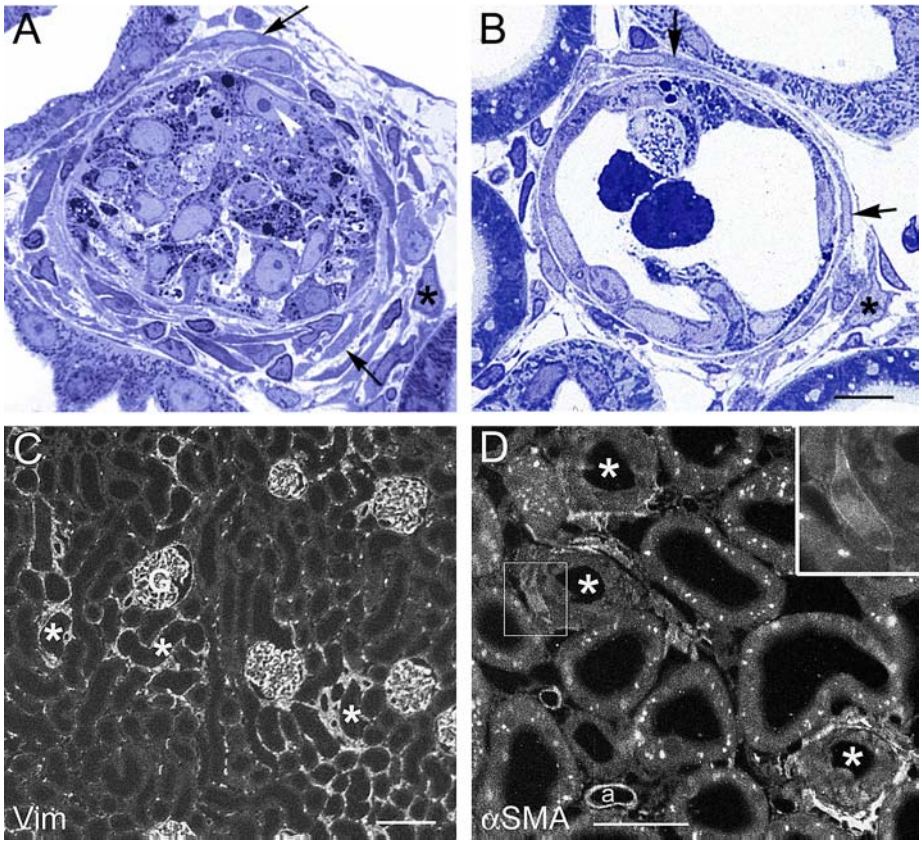

Fig. 1 Focal peritubular inflammation associated with injured distal tubules in thiazide-treated rats. **a, b** 1-μm Epon sections, **c, d** cryostat sections. **a** DCT profile after 3 days of thiazide-treatment. Disorganized epithelial cells fill the tubular lumen; one of the apoptotic cells within the tubular lumen is indicated by a *white arrowhead*; the tubular profile is surrounded by enlarged fibroblasts (*asterisk*), fusiform cells (*arrows*), and small mononuclear cells. **b** DCT profile after 4 days of thiazide-treatment. The tubular lumen is lined by simple flat cells with large, light cell nuclei; epithelial cells desquamate into the tubular lumen; peritubular cells adjacent to the diseased tubule reveal fusiform profiles (*arrows*). The *asterisk* indicates an enlarged fibroblast; *bars* **a, b** ~10 μm. **c** Three days of treatment: overview of renal cortex; immunofluorescence for vimentin (*Vim*); injured DCT profiles (*asterisks*) are revealed by the focal peritubular accumulations of vimentin-positive cells. *G* glomeruli, *bar* ~100 μm. **d** Three days of treatment: immunofluorescence for αSMA. Injured distal tubular profiles (*asterisks*) display thickened epithelial lining and are surrounded by thick layers of αSMA; arteriole *a* with αSMA-positive wall. *Insert* higher magnification of the area outlined in the figure, showing a peritubular αSMA-positive cell in anaphase of mitosis, *bar* ~50 μm

The inflamed peritubular interstitium contains myofibroblasts

Myofibroblasts differ from peritubular fibroblasts in healthy kidneys among others by upregulation of the intermediate filament protein vimentin and of αSMA (Fig. 2).

The intermediate filament protein vimentin is regarded as a marker for cells of mesenchymal origin and is expressed in migrating cells, including mononuclear cells. Stromal cells in the kidneys of newborn rats express both vimentin and αSMA (Marxer-Meier et al. 1998). Both proteins become undetectable in peritubular stromal cells during the first two postnatal weeks, whereas 5′NT-expression in their plasma membrane progressively appears (Marxer-Meier et al. 1998).

After 3 days of thiazide treatment (Fig. 2a) the cytoplasm of 5′NT-positive cells close to injured tubules showed weak-to-moderate immunoreactivity for vimentin. Small oval and round, heavily vimentin-positive (but 5′NT negative) cell profiles were frequently seen in intimate contact with 5′NT-positive fibroblasts. They probably represented mononuclear cells. The damaged epithelium of the DCT also revealed very weak, diffuse staining for vimentin.

After 4 days of treatment (Fig. 2b) the cells around diseased distal tubules formed multi-layered sheaths of fusiform cells, outlined by 5′NT, and with weak, but distinct, cytoplasmic staining for vimentin. Stellate 5′NT-positive cells in the periphery of the sheaths expressed vimentin as well. Vimentin is well apparent also in the now low DCT cells, mainly along their basolateral plasma membranes (Fig. 2b).

Alpha SMA is regarded as a molecular marker for myofibroblasts (Desmouliere et al. 2003; Kalluri and Neilson 2003). After 4 days of treatment with thiazide, αSMA-positive cells closely surrounded injured DCTs (Fig. 2c). The plasmalemma of the αSMA-positive cells displayed 5′NT (Fig. 2c insert).

The presence of vimentin and αSMA in 5′NT-positive cells, together with their morphology, identified these

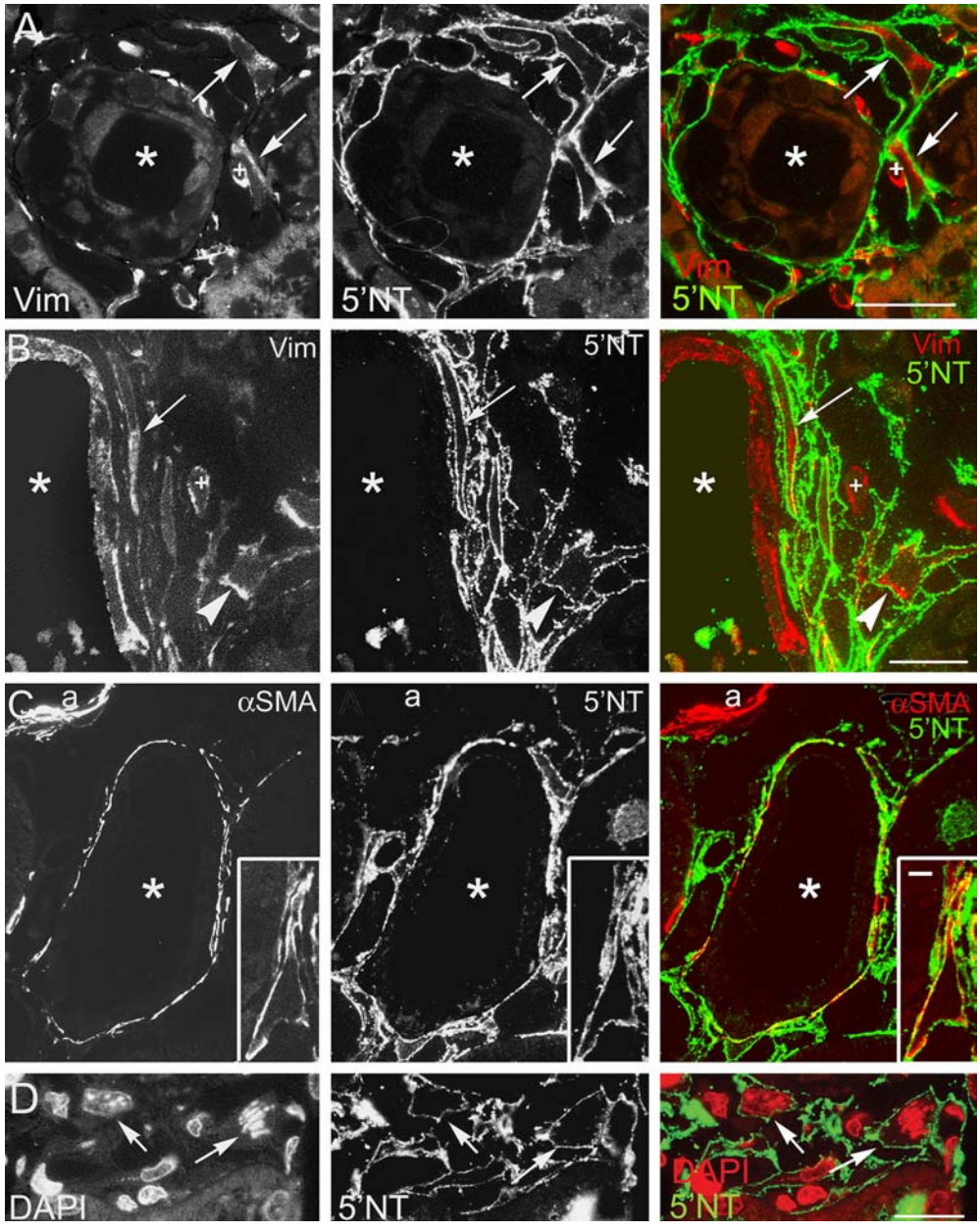

Fig. 2 The inflamed peritubular interstitium contains myofibroblasts. 1-μm cryostat sections, double immunofluorescence for vimentin and 5′NT (**a, b**), for αSMA and 5′NT (**c**), and for 5′NT and DNA, stained by DAPI (**d**). **a** Three days of thiazide treatment: vimentin is apparent in enlarged 5′NT-outlined cell profiles (*arrows*) in the vicinity of injured DCTs (*asterisk*). Heavy vimentin expression is detected in the cytoplasm of 5′NT-negative small, rounded cells (+) adjacent to the injured tubule. The epithelial cells reveal weak, diffuse, cytoplasmic staining for vimentin; *bar* ~20 μm. **b** Four days of thiazide treatment: vimentin is seen in fusiform cell profiles (*arrow*), closely adjacent to the diseased tubule and in 5′NT-outlined large stellate cell profiles (*arrowhead*). The epithelial cells are low and display vimentin along the basolateral plasma membranes and in the cytoplasm; *bar* ~20 μm. **c** Four days of thiazide treatment: αSMA in 5′NT-positive interstitial cells: the cells, co-expressing αSMA and 5′NT, completely and narrowly ensheath the injured tubules; *bar* ~20 μm. *Insert* higher magnification of a 5′NT/αSMA-positive cell; *bar* ~5 μm. **d** In the vicinity of diseased tubules pericarya of 5′NT-labeled fibroblasts rather frequently reveal mitotic figures, *left arrow* prophase, *right arrow* metaphase; *bar* ~10 μm

cells as (myo)fibroblasts. The 5′NT-positive cells close to damaged DCTs frequently revealed mitoses (Fig. 2d).

In order to assess a possible contribution of trans-differentiation of DCT cells to the genesis of myofibroblasts we investigated the distribution of FSP1. Indeed, the induction of FSP1 in injured proximal tubules has been taken as evidence of EMT (Chai et al. 2003; Ito et al. 2004; Iwano et al. 2002; Okada et al. 2000; Strutz and Neilson 2003). In addition to the antibodies against FSP1 (Strutz and Neilson 2003), willingly provided by F. Strutz, we also used a commercial antibody against S100A4. Of note is the fact that FSP1 and S100A4 are two names for the same protein (Barraclough 1998; Mazzucchelli 2002).

Anti-mouse FSP1 and anti-human S100A4 have identical binding patterns

In rats and mice both antibodies strongly bound to the cytoplasm of a subpopulation of peritubular cells, as well as to cells within the lumen of capillaries and venules (Fig. 3). In mice, FSP1/S100A4 consistently also stained endothelial cells of glomerular arterioles and of vasa recta. The anti-FSP1 antibody in rats and mice yielded markedly higher cytoplasmic background staining than the anti-S100A4 antibody. Moreover, in rats, some tubular luminal membranes were labeled with anti-FSP1 but not with antiS100A4 (not shown).

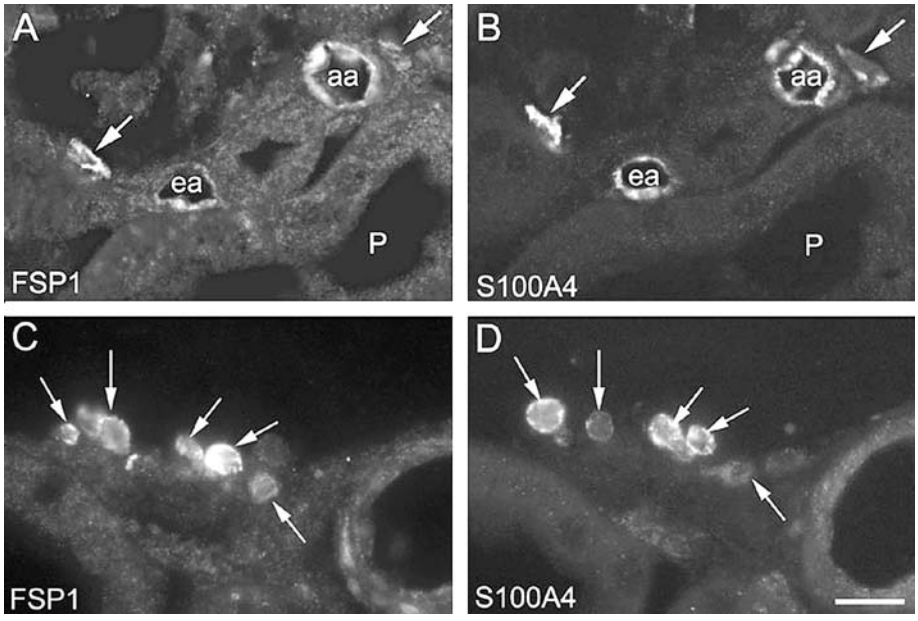

Fig. 3 Binding patterns of anti-FSP1 and anti-S100A4 are identical. Consecutive cryostat sections of mouse (**a, b**) and rat (**c, d**) kidney cortex. The distribution pattern of proteins, recognized by the antibodies, is identical. In both species the antibodies reveal interstitial cells (*arrows* in **a, b**) and mononuclear cells within the lumen of blood vessels (**c, d**; identical cells are indicated by *arrows*). In the mouse (**a, b**) both antibodies label glomerular arterioles. *aa* afferent arteriole, *ea* efferent arteriole). Immunolabeling with FSP1 (**a, c**) yields rather coarse background staining over all epithelia and interstitial cells. *Bar* ~10 μm

FSP1/S100A4and 5′NT are located in separate cells

In healthy kidneys and healthy regions of treated rats FSP1/S100A4-positive cells are sparse (Fig. 4a). After 3–4 days of treatment FSP1/S100A4-positive cells had accumulated in the peritubular space adjacent to injured distal tubular profiles (Fig. 4a). The pericaryon of FSP1/S100A4-positive cells showed an oval profile with a few processes close to healthy (Fig. 4b) and diseased (Fig. 4c) tubules. The pericaryon of fibroblasts in healthy cortical interstitium (Fig. 4b) has a characteristic sharp outline, and the delicate 5′NT-outlined fibroblast processes extend throughout the interstitial spaces (Fig. 4a,b).

After 3 days (Fig. 4c) the 5′NT-labeled cells reveal large, angular outlines, and fusiform profiles after 4 days (Fig. 4d) of treatment. In healthy as well as in diseased peritubular areas, 5′NT and FSP1/S100A4 were found in very close spatial association. However, they were consistently and clearly located in separate cells.

FSP1/S100A4 but not αSMA is detected in injured DCTs; FSP1/S100A4 and αSMA are located in separate peritubular cells

In 5-μm sections the damaged DCT epithelium reveals, after 3 days of treatment, faint immunostaining for FSP1/S100A4 but not for αSMA-(Fig. 5a). FSP1/S100A4-positive cells and αSMA-positive cells are accumulated around diseased DCTs. In 1-μm cryostat sections (Fig. 5b) the different identities of FSP1/S100A4-positive and αSMA-positive cells are evident. Thus, in the present model of inflammation, FSP1/S100A4 was not co-localized with αSMA and was not detected either in fibroblasts or in myofibroblasts.

FSP1/S100A4 recognizes mononuclear cells in the rat kidney

In order to disclose the nature of the FSP1/S100A4-positive cells in the peritubular space we made costainings for FSP1/S100A4 and markers for mononuclear cells. Under inflammatory conditions these cells migrate from the vasculature to the site of tubular lesion (Fig. 6).

In rats the frequency of cells expressing the common leukocyte antigen CD45 was markedly increased in the surroundings of diseased tubules (Fig. 6a). The large majority of FSP1/S100A4-positive cells in the interstitial space, as well as in the blood vessels (Fig. 6b), displayed CD45 in their plasma membrane (Table 2).

We also performed double labeling for FSP1/S100A4 and MHC class II. The latter is highly up-regulated in interstitial dendritic cells under peritubular inflammation, and their architecture (e.g., long cellular processes) slightly resembles that of peritubular fibroblasts. In the rat, FSP1/S100A4 and MHC class II were seldom seen in the same cells (not shown).

The data show that, in the rat, FSP1/S100A4 is expressed by a subclass of mononuclear cells within the vasculature as well as within the peritubular interstitium.

FSP1/S100A4 is expressed in lymphocytes in healthy and inflamed renal interstitium in mice

The claim that FSP1/S100A4 in renal tissue is specific for fibroblasts/myofibroblasts is grounded on studies in mice. Thus, it was mandatory to control whether the association of FSP1/S100A4 with mononuclear cells might be rat-specific. Therefore, we included in our study kidneys of untreated mice and of mice with glomerulonephritis. We carried out double labeling of FSP1/S100A4 with MHC class II, expressed in

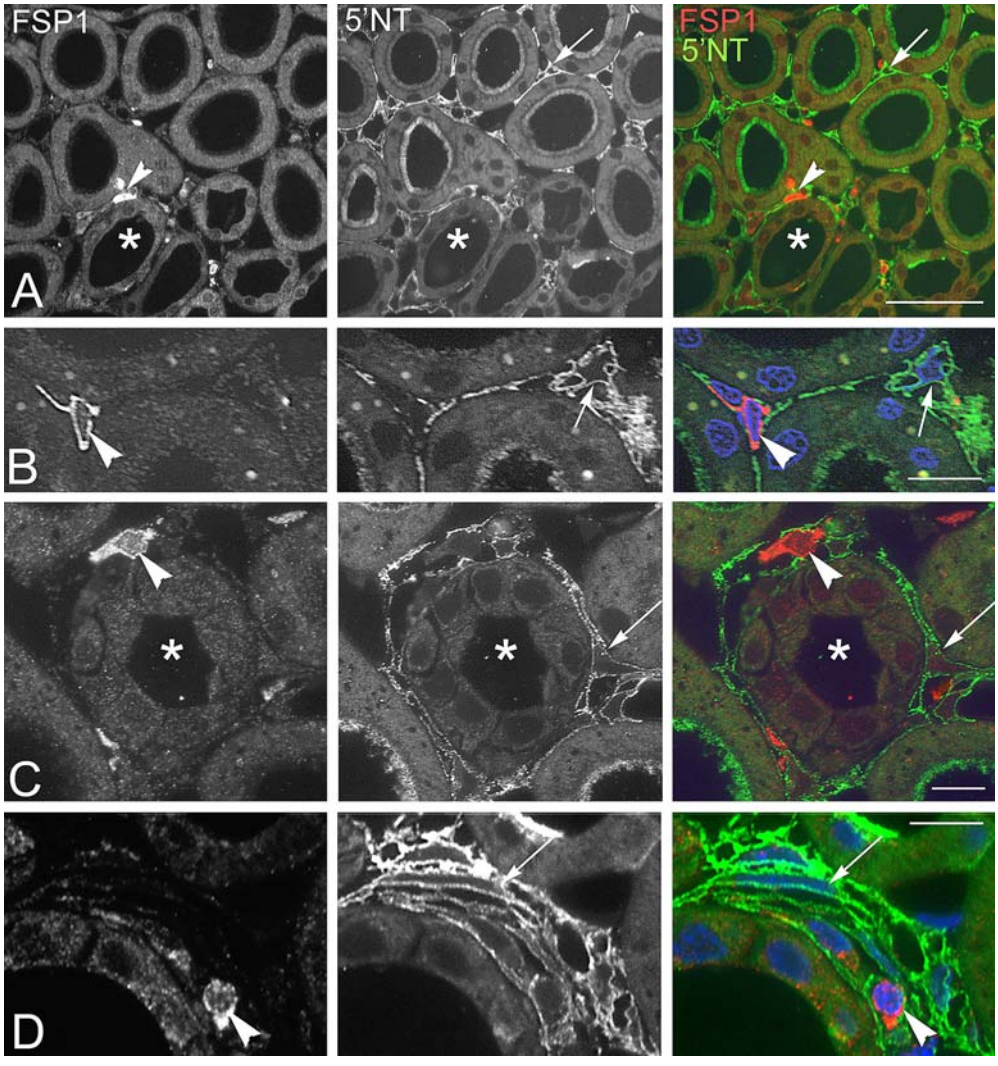

Fig. 4 FSP1/S100A4 and interstitial 5′NT are expressed by separate cell populations. **a** Cryostat sections, **b–d** 1-μm-thick cryostat sections of renal cortex after thiazide treatment; double immunofluorescence for FSP1/S100A4 and 5′NT; nuclei in **b** and **d** are stained by DAPI. **a** Overview, showing healthy and diseased cortical regions after 4 days of thiazide treatment. In healthy regions, interstitial FSP1/S100A4-positive cells are scarce; in the vicinity of injured DCTs (*asterisk*) their frequency is increased. Peritubular 5′NT-positive cells are present throughout the cortex; *bar* ~50 μm. **b** Higher magnification of a FSP1/S100A4-positive cell (*arrowhead*) and a 5′NT-positive peritubular cell (*arrow*) in healthy interstitium. FSP1/S100A4 is weakly detectable in the nucleus and strongly in the cytoplasm of the pericaryon and the few processes. 5′NT labels the plasma membrane of stellate cells and their extensive, delicate processes, extending between tubules and capillaries. **c** Three days of thiazide treatment: the pericarya of 5′NT-positive cells (*arrow*) surrounding diseased distal tubules (*asterisk*) display simplified outlines; their processes enclose FSP1/S100A4-positive cells. There is no cellular co-localization of FSP1/S100A4 and 5′NT. **d** Four days of thiazide-treatment: the 5′NT-labeled cells (*arrow*) adjacent to the diseased tubule reveal fusiform profiles; their processes narrowly enclose FSP1/S100A4-positive cells (*arrowhead*); *bars* (**b–d**) ~10 μm

macrophages, dendritic cells and B cells, or with the T cell-specific antigens CD3, CD4 and Thy 1 (CD90). It must be noted that the pan-T cell marker Thy 1 can be expressed in fibroblasts (Haeryfar and Hoskin 2004). However, the morphology of Thy 1-positive cells in mouse kidneys was incompatible with their identification as fibroblasts (Fig. 6). FSP1/S100A4 co-localized to various extents with the four leukocyte markers (Table 2, Fig. 7).

These data show that in mice, as in rats, at least a large fraction of the FSP1/S100A4-expressing cells are cells of the immune system rather than fibroblasts.

Discussion

The original aim of the present study was to investigate the interstitial inflammation and fibrosis in a model of distal tubular injury. Antibodies against "fibroblast specific protein 1" (FSP1/S100A4) were used in order to reveal whether EMT occurs in that model. We observed discrepancies between the immunofluorescence pattern of FSP1/S100A4 and the known shape and distribution of fibroblasts in the kidney. Since FSP1/S100A4 is used for the identification of fibroblasts in tissue sections (see below) and for targeting of fibroblasts in transgenic

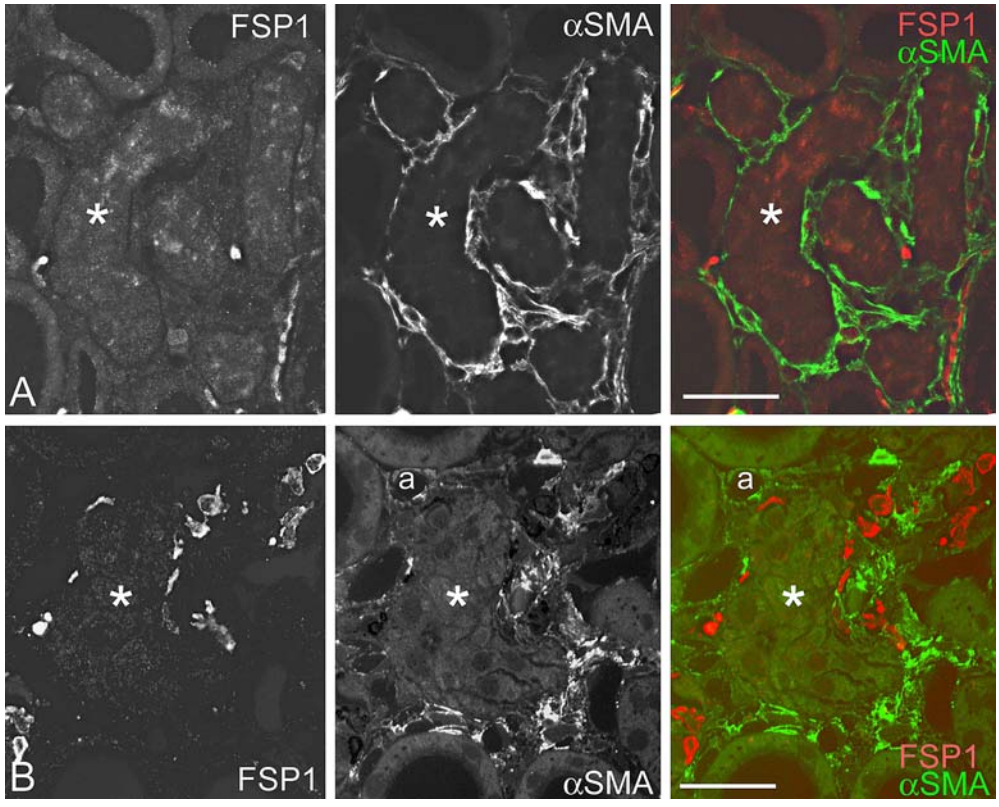

Fig. 5 FSP1/S100A4, but not αSMA, is detected in injured DCTs. Peritubular αSMA is not co-localized with FSP1/S100A4. **a** Cryostat section, **b** 1-μm-thick cryostat section; double immunofluorescence for FSP1/S100A4A and αSMA, 3 days of thiazide treatment. **a** the diseased distal tubules (*asterisks*) reveal diffuse cytoplasmic staining for FSP1/S100A4 and are surrounded by interstitial αSMA-positive cells, among which FSP1/S100A4-positive cells are interspersed. **a** Arteriole with αSMA-positive wall; *bar* ~60 μm. **b** Higher resolution in a 1-μm-thick section clearly shows the separate cellular locations of FSP1/S100A4A and αSMA; *bar* ~30 μm

manipulations (Bhowmick et al. 2004; Lawson et al. 2004; Okada et al. 2003) it appeared crucial to better characterize the cells that express that protein in the renal interstitium.

Treatment of rats with thiazide diuretics, which inhibit specifically the Na-Cl co-transporter in the DCT (Reilly and Ellison 2000), induces, within 3 days, dedifferentiation and degeneration of the DCT exclusively. We had previously observed that this tubular injury was accompanied by infiltration of inflammatory cells and accumulation of fibroblasts in the direct vicinity of the DCT (Loffing et al. 1996). This was confirmed in the present study. In addition we identified, in the inflamed area, myofibroblasts, on account of their expression of αSMA and vimentin. Together, these structural alterations constitute early signs of interstitial nephropathy.

The epithelial organization of the DCT appears to be largely lost during the first days of thiazide treatment. This is particularly striking on day 3 and goes along with the formation of sheaths of fibroblasts around the DCT. These observations prompted us to consider the possibility that epithelial cells might be transformed into fibroblasts or myofibroblasts. Indeed, recent studies

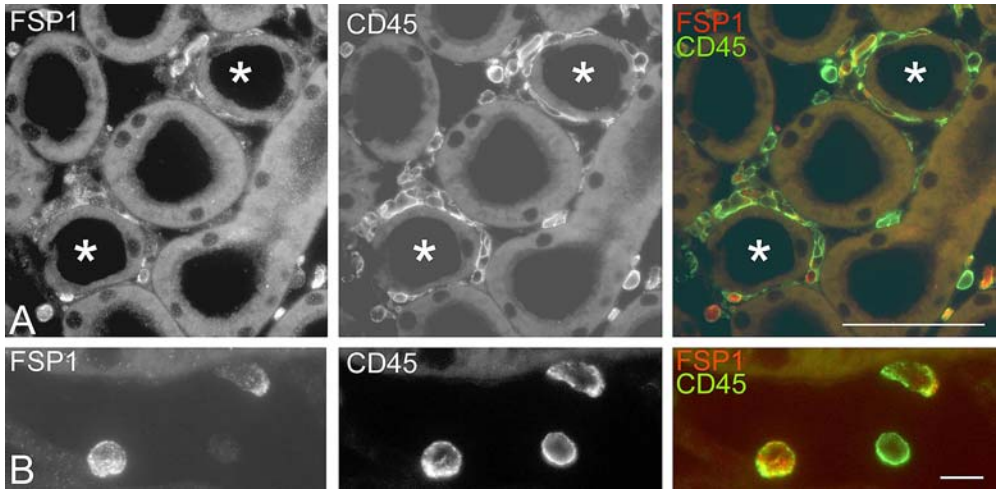

Fig. 6 FSP1/S100A4 recognizes mononuclear cells in rat kidney cryostat sections; double fluorescence for FSP1/S100A4 and CD45. **a** FSP1/S100A4-positive interstitial cells, accumulated around diseased distal tubules (*asterisks*), display CD45 in their plasma membrane; in a few CD45-positive cells FSP1/S100A4 was not detected. **b** Mononuclear cells within a capillary lumen; the two FSP1/S100A4-labeled cells are labeled by CD45 as well; *bars* **a** ~50 μm, **b** ~10 μm

Table 2 Quantification of expression of leukocyte markers in FSP1-positive cells. The percentages of leukocyte marker-expressing cells within the FSP1-positive population are given. At least 80 FSP1-positive cells were evaluated in each of two rats and two mice. The rats were perfused on day 4 of metolazone treatment, the mice on day 6, after induction of glomerulonephritis

CD45/FSP1 Rat	CD3/FSP1 Mouse	Thy-1/FSP1 Mouse	CD4/FSP1 Mouse	MHC II/FSP1 Mouse
91%	55%	66%	54%	26%

suggest that transformation of epithelial cells into fibroblasts/myofibroblasts contributes decisively to fibrosis in various renal diseases (Iwano and Neilson 2004; Iwano et al. 2002; Jinde et al. 2001; Kalluri and Neilson 2003; Liu 2004; Ng et al. 1998; Okada et al. 2000; Strutz and Neilson 2003; Yang and Liu 2002).

The present model offers several advantages over other models of interstitial inflammation. First, the time of onset is determined precisely, and the time course of histological alterations is very reproducible. Second, the DCT is affected specifically. Because the fractional cortical volume of the DCT is less than 10% (Kaissling et al. 1985), the inflammation associated with DCT injury is focally restricted, in contrast to interstitial changes associated with primary proximal tubular injury. The fractional tubular volume of proximal tubules in the cortex is 70%–80% (Pfaller 1982). The focal restriction of interstitial changes allows comparisons with unaffected areas within the same kidney section, which is particularly helpful for the correct assessment of immunostaining. Third, the injury is not accompanied by a systemic disease like uremia or hypertension. Fourth, the tubular injury is fully reversible within days of discontinuation of metolazone administration (unpublished data).

Because expression of FSP1/S100A4 in injured tubules has been considered as a hallmark of EMT in kidney disease (Chai et al. 2003; Ito et al. 2004; Iwano et al. 2002; Okada et al. 2000; Strutz and Neilson 2003), we used anti-FSP1/S100A4 antibodies in order to detect EMT in our model of distal tubule-associated interstitial inflammation. Our protocol of fixation by vascular perfusion provides patent interstitial spaces and enables clear distinction between peritubular cells. Furthermore, where needed, we improved the spatial resolution by using thin (1 μm) cryostat sections, allowing unequivocal attribution of a given labeling to a single cell or a cell process.

With this model we observed an accumulation of FSP1/S100A4-positive cells in the peritubular interstitium surrounding injured DCT profiles. To our surprise however, the antibody did not appear to label fibroblasts or myofibroblasts, since it did not co-localize in the same cells with 5′NT, recognizing cortical peritubular fibroblasts (Kaissling and Le Hir 1994), or with αSMA,

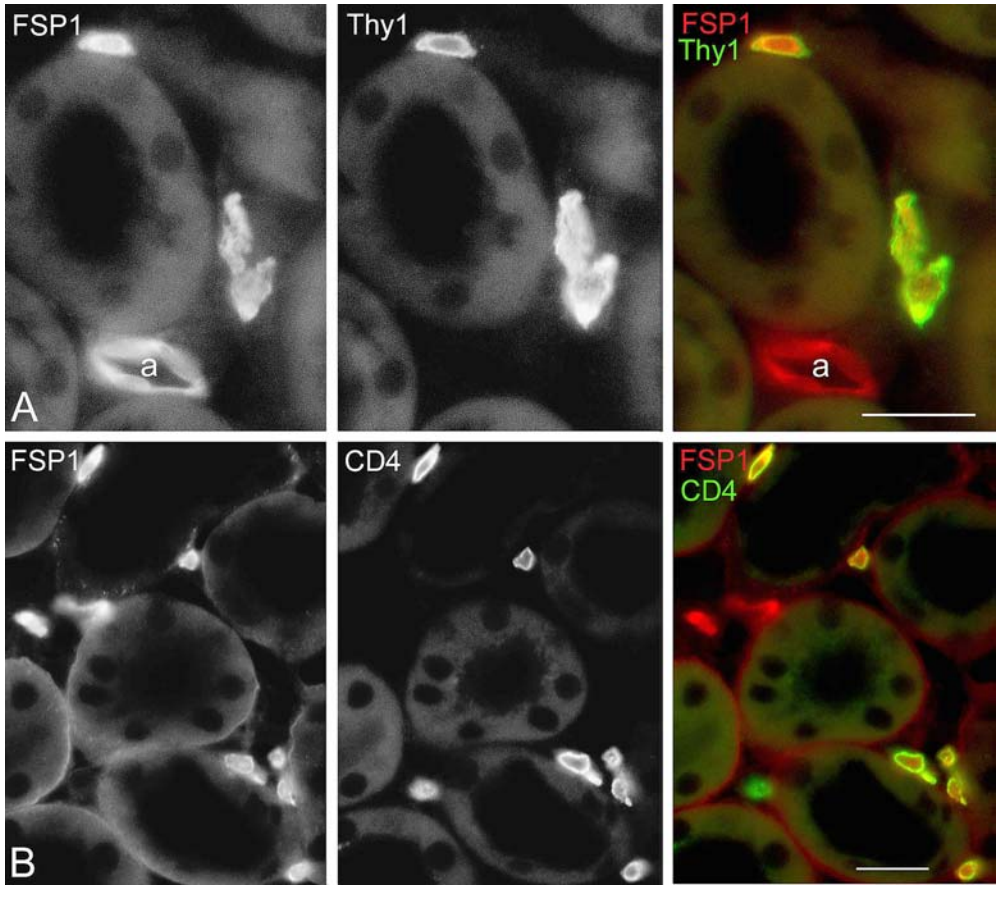

Fig. 7 FSP1/S100A4 is expressed in lymphocytes in healthy and inflamed renal interstitium in mice. Cryostat sections of mouse kidneys from healthy (**a**) and glomerulonephritic (**b**) mice. **a** Double immunofluorescence for FSP1/S100A4 and Thy 1; the present FSP1/S100A4-positive interstitial cells reveal Thy 1. FSP1/S100A4 is also detected in endothelial cells of arterioles (*a*); *bar* ~20 μm. **b** Double immunofluorescence showing a high level of co-localization of FSP1/S100A4 and CD4; *bar* ~10 μm

considered as molecular marker for myofibroblasts (Alpers et al. 1994; Desmouliere, et al. 2003; Kalluri and Neilson 2003; Pichler et al. 1996). The vast majority of FSP1/S100A4-positive cells were identified as leucocytes on the basis of three criteria: (1) in healthy as well as in inflamed areas some FSP1/S100A4+ cells were found in the lumen of peritubular blood vessels; (2) their morphology within the vascular as well as within the interstitial space was reminiscent of mononuclear cells and different from that of fibroblasts and myofibroblasts, and (3) in rats almost all FSP1/S100A4-positive cells displayed CD45, a surface molecule of mononuclear cells, in their plasma membrane. In kidneys of healthy and of glomerulonephritic mice (Le Hir and Besse-Eschmann 2003) roughly half of the FSP1/S100A4+ cells expressed CD3, CD4 or Thy 1, three T cell-specific proteins, and a few expressed MHC class II, which is found in B cells and macrophages.

The immunoreactivity for FSP1/S100A4 in leucocytes in the present study is compatible with previously published data. S100A4 is a calcium-binding protein that associates with the cytoskeleton and might play a role in cell motility (Barraclough 1998; Mazzucchelli 2002). It has been detected in lymphocytes, macrophages and granulocytes (Barraclough 1998; Mazzucchelli 2002; Taylor et al. 2002). A fraction of the FSP1/S100A4-positive cells in the kidney of rats after ureteral obstruction were identified as inflammatory cells according to their morphology (Ito et al. 2004). The low incidence of FSP1/S100A4+ cells in the healthy renal interstitium, and their increase in inflammatory lesions, is explained by the fact that leukocytes are rare in healthy kidneys but frequent in diseased ones.

Besides leukocytes, FSP1/S100A4 has been found in osteoblasts (Duarte et al. 2003), in chondrocytes (Mazzetti et al. 2004) and in subpopulations of glial cells and neurons (Sandelin et al. 2004) as well as in various tumors (Barraclough 1998; Mazzucchelli 2002; Taylor et al. 2002). Thus, whereas it has been found in fibroblasts in the regenerating cornea (Ryan et al. 2003) and in the inflamed synovia (Masuda et al. 2002), FSP1/S100A4 is clearly not a fibroblast-specific protein, as suggested by its name.

Fibroblasts of the peritubular interstitium of the rat kidney express 5′NT (Dawson et al. 1989; Gandhi et al. 1990; Kaissling et al. 1996; Kaissling and Le Hir 1994; Le Hir and Kaissling 1989). The lack of cellular colocalization of 5′NT and FSP1/S100A4, as well as the different morphologies of the 5′NT-labeled and FSP1/S100A4-labeled cells in the renal peritubular interstitium, show that rodent kidney fibroblasts in vivo are not recognized by the FSP1/S100A4 antibodies. Likewise, in the present study, the αSMA-expressing and vimentin-expressing myofibroblasts, which accumulate in the inflamed renal interstitium, display 5′NT.

Previous conclusions about the incidence of fibroblasts in the kidney on the basis of immunolabeling with anti-FSP1 (Chai et al. 2003; Ito et al. 2004; Iwano et al. 2002; Okada et al. 2000; Spurgeon et al. 2004; Vielhauer et al. 2004) or anti-S100A4 (Ito et al. 2004; Basile et al. 2005) must be reconsidered. The scarcity of FSP1-positive cells in the normal kidney has been interpreted as indication of a low incidence of fibroblasts (Iwano et al. 2002; Okada et al. 2000; Strutz and Neilson 2003). However, morphological studies had unequivocally established the widespread and regular occurrence of fibroblasts in the peritubular interstitium of the healthy kidney (Bulger and Nagle 1973; Kaissling and Le Hir 1994; Lemley and Kriz 1991). The functional roles of fibroblasts within the peritubular space of healthy kidneys are, among many others, the production of extracellular matrix in the form of fibers (Lemley and Kriz 1991) and, in cortical peritubular fibroblasts, the synthesis of renal erythropoietin (Bachmann et al. 1993). Owing to their strategic position between tubules and vessels and their extensive contact with all other interstitial cells, the peritubular fibroblasts may receive signals from all tissue components and respond to them in an integrative manner, e.g., in the case of fibrogenic signals they may produce increased amounts of matrix and become transformed to myofibroblasts.

At present it is difficult to speculate on the significance of the immunoreactivity for FSP1/S100A4 in tubules in some renal diseases. Indeed, a variety of functions has been attributed to this protein (Barraclough 1998; Mazzucchelli 2002; Taylor et al. 2002). Moreover, in inflammatory environments, tubular cells can up-regulate a variety of proteins that are normally found in cells of the immune system, for instance, MHC class II (Takei et al. 2000), B7 (Niemann-Masanek et al. 2002), CD14 (Fearns et al. 1995; Morrissey et al. 2000), CD44 (Wuthrich 1992) and CD40 (Hong et al. 2002; van Kooten et al. 2000). Also, cytoskeletal proteins, such as vimentin, may be up-regulated in regenerating renal epithelial cells (Witzgall et al. 1994; Zhu et al. 1996). This up-regulation might be associated with cell spreading and cell motility along denuded basement membrane after epithelial desquamation (Zhu et al. 1996). Interestingly, S100A4 plays a role in the induction of cell motility (Barraclough 1998; Mazzucchelli 2002).

Expression of αSMA in tubular cells has been used as more evidence of EMT in renal diseases (Jinde et al. 2001; Li et al. 2003; Ng et al. 1998; Yang and Liu 2001; Yang and Liu 2002). In the present study, αSMA was not detected in tubular cells. In view of the present data, it is likely that myofibroblasts in the inflamed regions originated from resident interstitial fibroblasts. The fact that, in this early stage of interstitial disease, all αSMA-positive interstitial cells were 5′NT-positive, like the peritubular fibroblasts, is in agreement with this proposal. The high frequency of mitotic figures in fibroblasts and myofibroblasts in the periphery of injured DCTs corroborates the former suggestions that local proliferation accounts for the accumulation of these cells (Desmouliere et al. 2003).

In conclusion, FSP1 is not a ‘‘fibroblast-specific antigen’’ as suggested by its name. Hence, immunolabeling for FSP1 does not provide information about the

contribution of EMT to the accumulation of (myo)fibroblasts in inflamed areas of the renal interstitium. Our data suggest that, in a model of distal tubular injury, fibroblasts are transformed into myofibroblasts and that both cell types proliferate.

Acknowledgments We are grateful to Dr. Frank Strutz for providing us with a sample of anti-FSP1 antibodies. We thank Lea Kläusli for technical assistance.

References

Abbate M, Zoja C, Rottoli D, Corna D, Tomasoni S, Remuzzi G (2002) Proximal tubular cells promote fibrogenesis by TGF-beta1-mediated induction of peritubular myofibroblasts. Kidney Int 61:2066–2077

Alpers CE, Hudkins KL, Floege J, Johnson RJ (1994) Human renal cortical interstitial cells with some features of smooth muscle cells participate in tubulointerstitial and crescentic glomerular injury. J Am Soc Nephrol 5:201–209

Bachmann S, Le Hir M, Eckardt KU (1993) Co-localization of erythropoietin mRNA and ecto-5′-nucleotidase immunoreactivity in peritubular cells of rat renal cortex indicates that fibroblasts produce erythropoietin. J Histochem Cytochem 41:335–341

Barraclough R (1998) Calcium-binding protein S100A4 in health and disease. Biochim Biophys Acta 1448:190–199

Basile DP, Fredrich K, Alausa M, Vio CP, Liang M, Rieder MR, Green AS, Cowley AW Jr (2005) Identification of persistently altered gene expression in kidney following functional recovery from ischemic renal failure. Am J Physiol Renal Physiol 288:F953–F963

Bhowmick NA, Chytil A, Plieth D, Gorska AE, Dumont N, Shappell S, Washington MK, Neilson EG, Moses HL (2004) TGF-beta signaling in fibroblasts modulates the oncogenic potential of adjacent epithelia. Science 303:848–851

Bulger RE, Nagle RB (1973) Ultrastructure of the interstitium in the rabbit kidney. Am J Anat 136:183–203

Chai Q, Krag S, Chai S, Ledet T, Wogensen L (2003) Localisation and phenotypical characterisation of collagen-producing cells in TGF-beta 1-induced renal interstitial fibrosis. Histochem Cell Biol 119:267–280

Dawson TP, Gandhi R, Le Hir M, Kaissling B (1989) Ecto 1-5′-nucleotidase: localization in rat kidney by light microscopic histochemical and immunohistochemical methods. J Histochem Cytochem 37:39–47

Desmouliere A, Darby IA, Gabbiani G (2003) Normal and pathologic soft tissue remodeling: role of the myofibroblast, with special emphasis on liver and kidney fibrosis. Lab Invest 83:1689–1707

Diamond JR, van Goor H, Ding G, Engelmyer E (1995) Myofibroblasts in experimental hydronephrosis. Am J Pathol 146:121–129

Duarte WR, Shibata T, Takenaga K, Takahashi E, Kubota K, Ohya K, Ishikawa I, Yamauchi M, Kasugai S (2003) S100A4: a novel negative regulator of mineralization and osteoblast differentiation. J Bone Miner Res 18:493–501

El-Nahas AM (2003) Plasticity of kidney cells: role in kidney remodeling and scarring. Kidney Int 64:1553–1563

Fearns C, Kravchenko VV, Ulevitch RJ, Loskutoff DJ (1995) Murine CD14 gene expression in vivo: extramyeloid synthesis and regulation by lipopolysaccharide. J Exp Med 181:857–866

Gandhi R, Le Hir M, Kaissling B (1990) Immunolocalization of ecto-5′-nucleotidase in the kidney by a monoclonal antibody. Histochemistry 95:165–174

Haeryfar SMM, Hoskin DW (2004) Thy-1: More than a mouse pan-T cell marker. J Immunol 173:3581–3588

Herzlinger D (2002) Renal interstitial fibrosis: remembrance of things past? J Clin Invest 110:305–306

Hong Y, Zhou W, Li K, Sacks SH (2002) Triptolide is a potent suppressant of C3, CD40 and B7h expression in activated human proximal tubular epithelial cells. Kidney Int 62:1291–1300

Ito K, Chen J, El Chaar M, Stern JM, Seshan SV, Khodadadian JJ, Richardson I, Hyman MJ, Vaughan ED Jr, Poppas DP, Felsen D (2004) Renal damage progresses despite improvement of renal function after relief of unilateral ureteral obstruction in adult rats. Am J Physiol Renal Physiol 287:F1283–F1293

Iwano M, Neilson EG (2004) Mechanisms of tubulointerstitial fibrosis. Curr Opin Nephrol Hypertens 13:279–284

Iwano M, Plieth D, Danoff TM, Xue C, Okada H, Neilson EG (2002) Evidence that fibroblasts derive from epithelium during tissue fibrosis. J Clin Invest 110:341–350

Jinde K, Nikolic-Paterson DJ, Huang XR, Sakai H, Kurokawa K, Atkins RC, Lan HY (2001) Tubular phenotypic change in progressive tubulointerstitial fibrosis in human glomerulonephritis. Am J Kidney Dis 38:761–769

Kaissling B, Le Hir M (1994) Characterization and distribution of interstitial cell types in the renal cortex of rats. Kidney Int 45:709–720

Kaissling B, Bachmann S, Kriz W (1985) Structural adaptation of the distal convoluted tubule to prolonged furosemide treatment. Am J Physiol 248:F374–F381

Kaissling B, Hegyi I, Loffing J, Le Hir M (1996) Morphology of interstitial cells in the healthy kidney. Anat Embryol (Berl) 193:303–318

Kalluri R, Neilson EG (2003) Epithelial–mesenchymal transition and its implications for fibrosis. J Clin Invest 112:1776–1784

Kang Y, Massague J (2004) Epithelial–mesenchymal transitions: twist in development and metastasis. Cell 118:277–279

van Kooten C, Woltman AM, Daha MR (2000) Immunological function of tubular epithelial cells: the functional implications of CD40 expression. Exp Nephrol 8:203–207

Lawson WE, Polosukhin VV, Zoia O, Stathopoulos GT, Han W, Plieth D, Loyd JE, Neilson EG, Blackwell TS (2004) Characterization of fibroblast specific protein 1 in pulmonary fibrosis. Am J Respir Crit Care Med 23:23

Le Hir M, Kaissling B (1989) Distribution of 5′-nucleotidase in the renal interstitium of the rat. Cell Tissue Res 258:177–182

Le Hir M, Besse-Eschmann V (2003) A novel mechanism of nephron loss in a murine model of crescentic glomerulonephritis. Kidney Int 63:591–599

Le Hir M, Keller C, Eschmann V, Hahnel B, Hosser H, Kriz W (2001) Podocyte bridges between the tuft and Bowman's capsule: an early event in experimental crescentic glomerulonephritis. J Am Soc Nephrol 12:2060–2071

Lemley KV, Kriz W (1991) Anatomy of the renal interstitium. Kidney Int 39:370–381

Li Y, Yang J, Dai C, Wu C, Liu Y (2003) Role for integrin-linked kinase in mediating tubular epithelial to mesenchymal transition and renal interstitial fibrogenesis. J Clin Invest 112:503–516

Liu Y (2004) Epithelial to mesenchymal transition in renal fibrogenesis: pathologic significance, molecular mechanism, and therapeutic intervention. J Am Soc Nephrol 15:1–12

Loffing J, Loffing-Cueni D, Hegyi I, Kaplan MR, Hebert SC, Le Hir M, Kaissling B (1996) Thiazide treatment of rats provokes apoptosis in distal tubule cells. Kidney Int 50:1180–1190

Marxer-Meier A, Hegyi I, Loffing J, Kaissling B (1998) Postnatal maturation of renal cortical peritubular fibroblasts in the rat. Anat Embryol (Berl) 197:143–153

Masuda K, Masuda R, Neidhart M, Simmen BR, Michel BA, Muller-Ladner U, Gay RE, Gay S (2002) Molecular profile of synovial fibroblasts in rheumatoid arthritis depends on the stage of proliferation. Arthritis Res 4:R8

Mazzetti I, Magagnoli G, Paoletti S, Uguccioni M, Olivotto E, Vitellozzi R, Cattini L, Facchini A, Borzi RM (2004) A role for chemokines in the induction of chondrocyte phenotype modulation. Arthritis Rheum 50:112–122

Mazzucchelli L (2002) Protein S100A4: too long overlooked by pathologists? Am J Pathol 160:7–13

Morrissey J, Guo G, McCracken R, Tolley T, Klahr S (2000) Induction of CD14 in tubular epithelial cells during kidney disease. J Am Soc Nephrol 11:1681–1690

Ng YY, Huang TP, Yang WC, Chen ZP, Yang AH, Mu W, Nikolic-Paterson DJ, Atkins RC, Lan HY (1998) Tubular epithelial–myofibroblast transdifferentiation in progressive tubulointerstitial fibrosis in 5/6 nephrectomized rats. Kidney Int 54:864–876

Niemann-Masanek U, Mueller A, Yard BA, Waldherr R, van der Woude FJ (2002) B7–1 (CD80) and B7–2 (CD 86) expression in human tubular epithelial cells in vivo and in vitro. Nephron 92:542–556

Okada H, Ban S, Nagao S, Takahashi H, Suzuki H, Neilson EG (2000) Progressive renal fibrosis in murine polycystic kidney disease: an immunohistochemical observation. Kidney Int 58:587–597

Okada H, Inoue T, Kanno Y, Kobayashi T, Watanabe Y, Ban S, Neilson EG, Suzuki H (2003) Selective depletion of fibroblasts preserves morphology and the functional integrity of peritoneum in transgenic mice with peritoneal fibrosing syndrome. Kidney Int 64:1722–1732

Pfaller W (1982) Structure function correlation on rat kidney. Quantitative correlation of structure and function in the normal and injured rat kidney. Adv Anat Embryol Cell Biol 70:1–106

Phan SH (2002) The myofibroblast in pulmonary fibrosis. Chest 122:286S–289S

Pichler RH, Hugo C, Shankland SJ, Reed MJ, Bassuk JA, Andoh TF, Lombardi DM, Schwartz SM, Bennett WM, Alpers CE, Sage EH, Johnson RJ, Couser WG (1996) SPARC is expressed in renal interstitial fibrosis and in renal vascular injury. Kidney Int 50:1978–1989

Reilly RF and Ellison DH (2000) Mammalian distal tubule: physiology, pathophysiology, and molecular anatomy. Physiol Rev 80:277–313

Ryan DG, Taliana L, Sun L, Wei ZG, Masur SK, Lavker RM (2003) Involvement of S100A4 in stromal fibroblasts of the regenerating cornea. Invest Ophthalmol Vis Sci 44:4255–4262

Sandelin M, Zabihi S, Liu L, Wicher G, Kozlova EN (2004) Metastasis-associated S100A4 (Mts1) protein is expressed in subpopulations of sensory and autonomic neurons and in Schwann cells of the adult rat. J Comp Neurol 473:233–243

Sartore S, Chiavegato A, Faggin E, Franch R, Puato M, Ausoni S, Pauletto P (2001) Contribution of adventitial fibroblasts to neointima formation and vascular remodeling: from innocent bystander to active participant. Circ Res 89:1111–1121

Short M, Nemenoff RA, Zawada WM, Stenmark KR, Das M (2004) Hypoxia induces differentiation of pulmonary artery adventitial fibroblasts into myofibroblasts. Am J Physiol Cell Physiol 286:C416–C425

Spurgeon KS, Donohoe DL, Basile DP (2004) Transforming growth factor-beta in acute renal failure: receptor expression, effects on proliferation, cellularity and vascularization after recovery from injury. Am J Physiol Renal Physiol 9:9

Strutz F, Neilson EG (2003) New insights into mechanisms of fibrosis in immune renal injury. Springer Semin Immunopathol 24:459–476

Strutz F, Okada H, Lo CW, Danoff T, Carone RL, Tomaszewski JE, Neilson EG (1995) Identification and characterization of a fibroblast marker: FSP1. J Cell Biol 130:393–405

Takei Y, Sims TN, Urmson J, Halloran PF (2000) Central role for interferon-gamma receptor in the regulation of renal MHC expression. J Am Soc Nephrol 11:250–261

Taylor S, Herrington S, Prime W, Rudland PS, Barraclough R (2002) S100A4 (p9Ka) protein in colon carcinoma and liver metastases: association with carcinoma cells and T-lymphocytes. Br J Cancer 86:409–416

Thiery JP (2002) Epithelial–mesenchymal transitions in tumour progression. Nat Rev Cancer 2:442–454

Vielhauer V, Berning E, Eis V, Kretzler M, Segerer S, Strutz F, Horuk R, Grone HJ, Schlondorff D, Anders HJ (2004) CCR1 blockade reduces interstitial inflammation and fibrosis in mice with glomerulosclerosis and nephrotic syndrome. Kidney Int 66:2264–2278

Witzgall R, Brown D, Schwarz C, Bonventre JV (1994) Localization of proliferating cell nuclear antigen, vimentin, c-Fos, and clusterin in the postischemic kidney. Evidence for a heterogenous genetic response among nephron segments, and a large pool of mitotically active and dedifferentiated cells. J Clin Invest 93:2175–2188

Wuthrich RP (1992) Intercellular adhesion molecules and vascular cell adhesion molecule-1 and the kidney. J Am Soc Nephrol 3:1201–1211

Yang J, Liu Y (2001) Dissection of key events in tubular epithelial to myofibroblast transition and its implications in renal interstitial fibrosis. Am J Pathol 159:1465–1475

Yang J, Liu Y (2002) Blockage of tubular epithelial to myofibroblast transition by hepatocyte growth factor prevents renal interstitial fibrosis. J Am Soc Nephrol 13:96–107

Zeisberg M, Strutz F, Muller GA (2001) Renal fibrosis: an update. Curr Opin Nephrol Hypertens 10:315–320

Zhu MQ, De Broe ME, Nouwen EJ (1996) Vimentin expression and distal tubular damage in the rat kidney. Exp Nephrol 4:172–183